Measuring Biophysical Forest Variables and Land Cover Mapping of Seyhan Watershed

Süha BERBEROĞLU[1], **Fatih EVRENDİLEK**[2], **and Sibel MEYDAN**[1]

[1]*Department of Landscape Architecture, University of Cukurova, Adana, Turkey*

[2]*Department of Landscape Architecture, Mustafa Kemal University, Hatay, Turkey*

e-mail: suha@cu.edu.tr

1. Introduction

There are strong relationship between the concentration of key biochemicals (e.g., nitrogen, lignin etc.) and the amount of radiation reflected from a vegetation canopy. Information on canopy biochemistry is of great importance for the study of nutrient cycling, productivity, vegetation stress and for input to ecosystem simulation models. Remotely sensed-data, Geographic Information Systems (GIS) and process-based simulation models have provided the capability to assess ecological change at broad spatio-temporal scales. Remotely sensed data recorded in visible and near infrared wavelengths can be used to estimate how much vegetation is present (e.g., biomass, leaf area index (LAI)) and the condition of that vegetation (e.g., concentration of nitrogen and lignin). Both vegetation amount and condition can be estimated over large areas of terrain and used to provide spatially explicit input to model of global primary production and nutrient cycling. A number of potential climate change and degradation issues in terrestrial environments have been identified and studied over the past decades. Various international committees (NASA, NOAA, ESA, NASDA etc.) have identified satellite remote sensing as a unique and essential tool to repetitively acquire global environmental data at spatial, temporal, radiometric and spectral resolutions appropriate to investigate these issues.

This study is motivated by changing patterns of land cover and the hypothetical linkages between these patterns, human activities, biogeochemical cycles and climate. Two major objectives of this study are (i) to quantify the biophysical forest variable, (ii) to detect changes among past and present LULC of Seyhan watershed. Forest variables including tree height, diameter at breast height (dbh) (1.30 cm), tree age, cover, abundance, slope, aspect, elevation, GPS coordinates, and amount and decomposition rate of litterfall were measured for five plots representing different forest stands. In the image processing section, Maximum Likelihood (ML) and Artificial Neural Network (ANN) classifiers were applied to a full Landsat Enhanced Thematic Mapper (ETM) image which was acquired on 5 May 2003 of Seyhan watershed, Turkey. Inputs to the classifications comprised (i) spectral data (ii) spatial data (texture measures derived on a per-pixel basis) (iii) Digital Elevation Model (DEM). All these measurements and processing will be linked to estimate biogeochemical processes in this type of forest ecosystem.

2. Quantifying Aboveground Biomass and Productivity of Forest Stands

The following variables were started to be measured at the location “Katran Çukuru”, in the Directorship domain of Forestry Management, Aladağ-Adana, for at least ten individuals from each species in a sample area of 400 m^2 for each of the five forest stands of (1) Crimean pine (*Pinus nigra*), (2) Cedar of Lebanon (*Cedrus libani*), (3) mixed Taurus fir [*Abies cilicica*], C. Libani, and P. nigra, (4) Callabrian pine (*Pinus brutia*) and (5) juniper (*Juniperus excelsa*): tree height, diameter at breast height (dbh) (1.30 cm), tree age, cover, abundance, slope, aspect, elevation, GPS coordinates, and amount and decomposition rate of litterfall. Characteristic values of each forest stand, and best fitted linear regression lines between tree diameter (cm) and tree height (m) are provided below (Tables 1 and 2).

Litter decomposition is one of the key biogeochemical processes in forest ecosystems (Swift *et al.,* 1979). Analysis of decomposition data by the fitting of mathematical models to estimate constants that describe the loss of mass overtime gives us considerable insight into the biology of global climate change (Tables 5 and 6). It is estimated that the nutrients released during litter decomposition can account for 69-87% of the total annual requirement of essential elements for forest plants (Waring and Schlesinger, 1985). One-mm meshed litter bags of 10 g dry weight needle leaf mass were collected from each of the five stands at their respective sampling dates, oven dried for 48 hrs at 60°C and weighed after a constant weight was obtained. The final weight represents the mass remaining after decay, and hence from this the percent of initial mass remaining was calculated. The percent of the initial mass remaining was plotted against time (days). The decomposition rate (*k*) of litterfall was calculated from the percentage of needle leaf litter mass remaining, using an exponential decay model (Jenny et al. 1949; Olson 1963) (Figure 1):

$$dM/dt = -kM$$

$$M_t = M_o * e^{-kt}$$

$$M_t/M_o = e^{-kt}$$

$$\ln (M_t/M_o) = -kt$$

$$k = -[\ln(M_t/M_o)]/t$$

where M_t: dry weight litter mass at a given time (t) expressed as a proportion of initial dry mass, M_o: initial dry weight litter mass, t: time, and *k*: the decay constant expressed in days^{-1}.

A negative exponential decay model assumes that a constant proportion of mass is lost over time. Half-life periods ($t_{0.5}$) of decomposing litter samples were estimated from *k* values, using the following equation (Bockheim *et al.*, 1991) (Tables 3 and 4):

$$t_{0.5} = \ln (0.05) / (-k) = 0.693 / (-k) \text{ in days}$$

Table 1. Simple linear regression models between the response variable of diameter (cm) at breast height (dbh) (1.30 cm) and explanatory variable of tree height (m) for the five forest stands in Katran Çukuru.

Forest stands	n	coefficient	slope	r^2 (%)	*p*
Pinus nigra	12	18.70	1.21	42	*
Cedrus libani	20	0.92	1.51	58	***
Mixed stand (*Abies cilicica-P. nigra-C. libani*)	36	1.89	1.69	50	***
Juniperus excelsa	25	1.08	3.01	38	**
Pinus brutia	21	12.8	2.42	27	*

*, **, and *** refer to $p < 0.05$, $p < 0.01$, and $p < 0.001$, respectively.

Table 2 Characteristic values (mean±SD) of forest stands in Katran Çukuru.

Species	height (m)	dbh (cm)	age (yr)	TBA ($m^2\ tree^{-1}$)	SBA ($m^2\ ha^{-1}$)	stem density ($stem\ ha^{-1}$)	Elevation (m)	aspect
Pinus nigra	22 ±4	45.6 ±8.1	92 ±14	0.168 ±0.060	50.4 ±17.9	300	1555	SW
Cedrus libani	20 ±6	31.5 ±11.3	114 ±7	0.087 ±0.062	43.6 ±30.8	500	1500	W
Mixed stand (*Abies cilicica-P. nigra-C. libani*)	13 ±5	23.2 ±11.7	103 ±6	0.053 ±0.053	47.4 ±47.7	900	1460	W
Juniperus excelsa	8 ±2	23.7 ±7.8	~100	0.049 ±0.28	30.4 ±17.7	625	1345	NW
Pinus brutia	19 ±2	33.5 ±11.6	~100	0.098 ±0.071	51.6 ±37.1	525	660	W

TBA: tree basal area; SBA: stand basal area; and dbh: diameter at breast height (1.30 m)

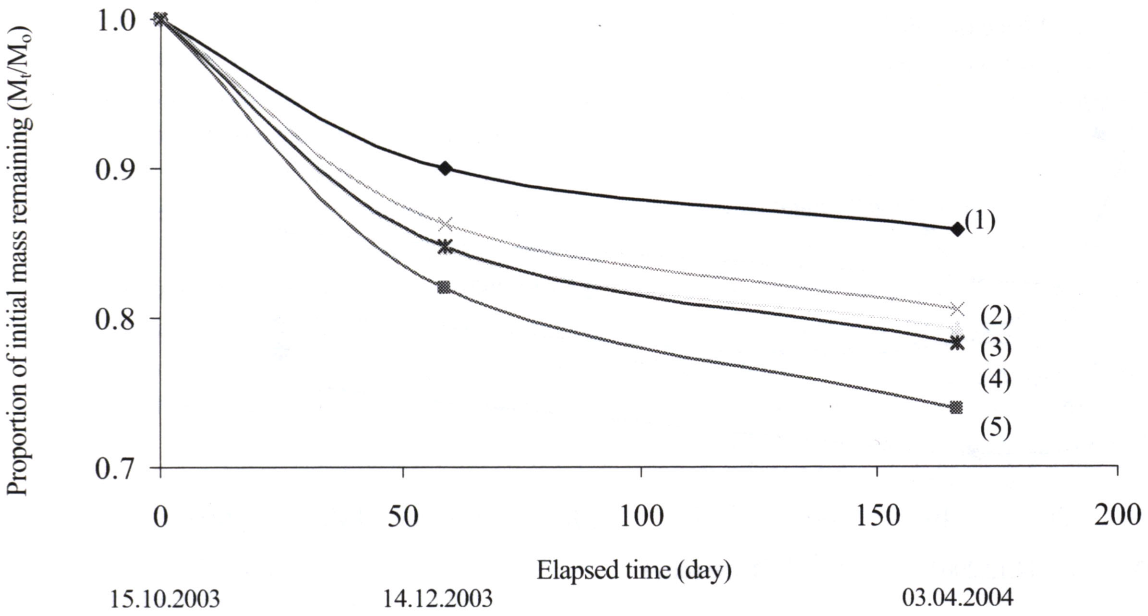

Figure 1 Proportion of dry-mass remaining as a function of time during decomposition of needle leaves in litterbags under five Mediterranean forest stands of (1) *Pinus nigra*, (2) *Pinus brutia*, (3) mixed *Abies cilicica-P. nigra-Cedrus libani*, (4) *Juniperus excelsa*, and (5) *Cedrus libani* in Katran Çukuru. Exponential decay models fitted are (1) $M_t/M_o = e^{-0.001x}$; (2) $M_t/M_o = e^{-0.0014x}$; (3) $M_t/M_o = e^{-0.0016x}$; (4) $M_t/M_o = e^{-0.0016x}$; and (5) $M_t/M_o = e^{-0.002x}$.

Table 3 Decomposition rates (*k*) and half-life times ($t_{0.5}$) for litters of the studied species in Katran çukuru of Seyhan Watershed (Adana, Turkey).

Forest stand
P. nigra
P. brutia
Mixed *Abies cilicica-P. nigra-Cedrus libani*
Juniperus excelsa
Cedrus libani

Values with the same superscript letter in the column "*k* (day^{-1}) are not significantly different at $p < 0.05$.

Table 4 Multiple comparisons of litter masses remaining under the five forest stands by one-way ANOVA.

Forest stand	Initial mass (g C)	Remaining mass (g C)		n
		day 59	day 167	
P. nigra	4.50	4.05±0.01a	3.86±0.09a	3
P. brutia	4.50	3.88±0.12ab	3.62±0.11b	3
Mixed *Abies cilicica-P. nigra-Cedrus libani*	4.50	3.80±0.01b	3.56±0.05b	3
Juniperus excelsa	4.50	3.81±0.08b	3.51±0.04b	3
Cedrus libani	4.50	3.68±0.09b	3.32±0.02c	3

Values with the same superscript letter in the columns "day 59" and "day 167" are not significantly different at $p < 0.01$ and $p < 0.001$, respectively.

Litterfall was collected from circular traps (0.25 m^2) located at each of the five forest stands at monthly intervals. The installation of litter traps was commenced on 15 October 2003. Litterfall from individual traps at each site was combined to give bulked samples for each component for each site for each collection period. Litterfall components consisted of leaves, reproductive structures (i.e. flowers, cones, and seeds), small woody material (i.e. bark, wood, and branches < 2 cm diameter), and unclassified material (i.e. any material passing through a 2 mm sieve). Before weighing for analysis, samples were dried until constant weight was achieved. In the cases where samples were lost at the sites, accession rates for that period were estimated as the average of accession rates directly preceding and following the missing data (Figure 2).

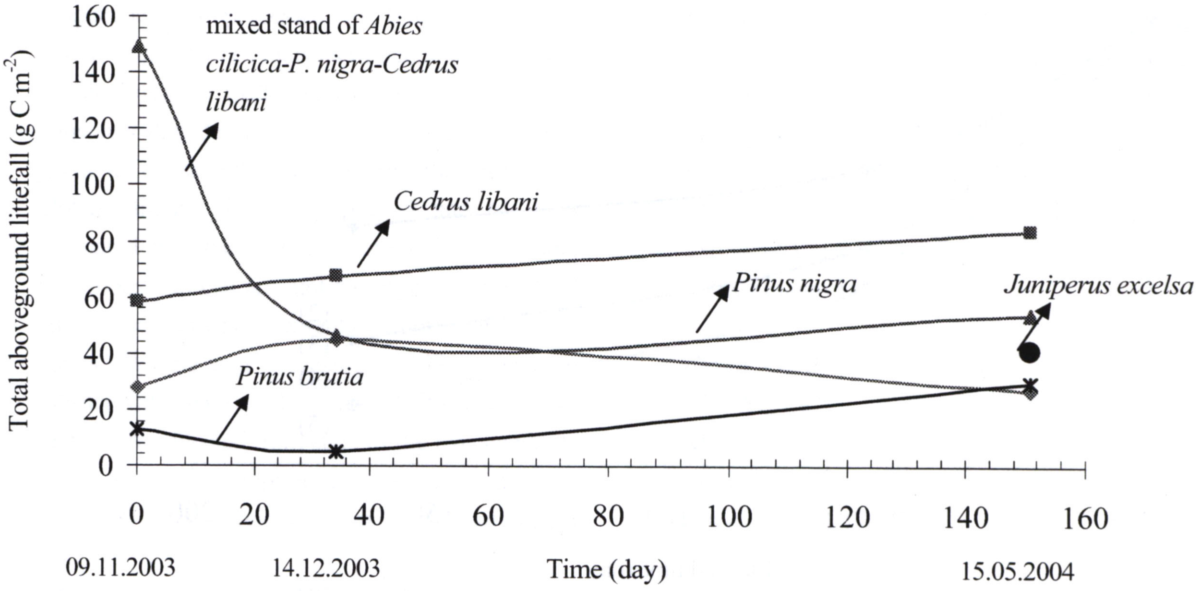

Figure 2 Total aboveground litterfalls (g C m^{-2}) (leaf + branch + seed + others) for five Mediterranean forest stands of (1) *Pinus nigra*, (2) *Pinus brutia*, (3) mixed *Abies cilicica-P. nigra-Cedrus libani*, (4) *Juniperus excelsa*, and (5) *Cedrus libani* in Katran Çukuru. Equations of best-fitted linear lines are (1) $y = -0.040x + 35.711$, $r^2 = 0.11$; (2) $y = 0.137x + 7.199$, $r^2 = 0.75$; (3) $y = -0.450x + 110.87$, $r^2 = 0.39$; and (5) $y = 0.165x + 59.739$, $r^2 = 0.98$.

3. Image Pre-processing and Classification of Land Use and Land Cover (LULC)

The aim of the classification is (1) to detect changes among past and present LULC of Seyhan watershed and (2) quantify soil organic C (SOC) pools and fluxes of CO_2 to the atmosphere. In so doing, the Landsat ETM image dated 5 May 2003 was geometrically corrected using nearest neighbour and geocoded to the Universal Transverse Mercator (UTM) co-ordinate system. Fifteen approximately evenly distributed ground control points (GCPs) were selected from the image.

The image was classified using ML and ANN classifiers and both spectral and textural information (from the variance and variogram) in per-pixel format. The ANN classification was performed using MATLAB software that simulated a feed-forward multi-layer perceptron model (MLP). The network architectures ranged from 6 to 12 input units (6 Landsat ETM sensor bands and, where relevant, textural measures). The first hidden layer included three times the number of input layer units. The network was trained with a learning rate of 0.01 and learning momentum of 0.5 as back-propagation requires small learning rates for stable learning. The network was trained until the root mean square error was minimised (gradient of the error at the outputs was less than 0.05), after 4000-8000 cycles. A sigmoid transfer function was utilised within the layers. The output was a hard classification, with only the code of the predicted class of membership indicated for each pixel.

Texture measures: All texture measures were extracted from the first principal component (Benediktsson & Sveinsson, 1997) of the six wavebands and these were used to create 'texture waveband(s)'. Then, per-pixel ML and ANN classifications were applied.

Variogram and variance: An algorithm based on the variogram computer code in the geostatistical software library GSLIB (Deutsch & Journel, 1992) was used to compute the variogram and variance. Variogram coefficients used as texture measures included (i) an approximation of variogram range, (ii) the semi-variance at various lags and (iii) variance. The variogram range was computed using two approximations; (i) the method of Ramstein & Raffy (1989) and (ii) the roots of the first derivative of a third-order polynomial fitted to the variogram. Both approximations were unstable in the first approach and this was because the semi-variance at large lags was computed from too few data and in the second approach this was because the small number of pixels in each window restricted the number of lags for which semi-variance could be computed. In many instances, very large ranges were estimated if the variograms did not reach a limit. Therefore, range was not employed in the analysis.

The texture measures derived from the average values of semi-variance at lags of 1, 2, 3, 4 and 5 pixels over a moving window. These texture measures provided additional information to the classifiers where the spectral discrimination of major land cover classes is subtle such as, settlement, bare soil (Table 5).

Table 5 The classification accuracy of using ANN with texture, DEM and spectral bands .

	ANN 6 bands + DEM + texture		
LAND COVERS	PA (%)	UA (%)	Kappa
Agriculture	85.71	90.41	0.8754
Bare ground	60.87	73.68	0.7174
Grassland	73.81	83.78	0.8145
Pinus brutia	76.60	80.00	0.7672
Pinus nigra	93.55	54.72	0.5008
Cedrus libani	14.29	50.00	0.4893
Abies sp.	59.00	18.20	0.1520
Water	90.70	97.50	0.9713
Wetland	66.67	100.00	1.0000
Settlement	75.00	75.00	0.7407
Snow	84.21	94.12	0.9376
Bulrush	100.00	56.25	0.5504
Sand	100.00	83.33	0.8255
Overall accuracy		**79.94**	

PA: Producer's Accuracy

UA: User's Accuracy

4. Discussion and Conclusions

Forest variables including tree height, diameter at breast height (dbh) (1.30 cm), tree age, cover, abundance, slope, aspect, elevation, GPS coordinates, and amount and decomposition rate of litterfall were measured for five plots representing different forest stands.

In the image processing and land cover mapping section, this study has integrated spectral, DEM and spatial information in the form of variogram by using ANN classifier with the aim of increasing the effectiveness of classification (by means of maximising the percentage accuracy) with which land cover can be classified. Synergy of the techniques mentioned above enabled more accurate classification and was useful where the spectral properties of the land cover classes was complex and overlapped in feature space.

5. References

Benediktsson, J.A. and Sveinsson, J.R., 1997. Feature extraction for multisource data classification with artificial neural networks. *International Journal of Remote Sensing;* 18:727-740.

Deutsch, C. and Journel, A. G., 1992. *GSLIB: Geostatistical Software Library and User's Guide.* Oxford University Press, New York.

Jenny, H., S. P. Gessel, and F.T. Bingham. 1949. Comparative study of decomposition of organic matter in temperate and tropical regions. Soil Science 68:419-432.

Olson, J. S. 1963. Energy storage and the balance of producers and decomposers in ecological systems. Ecology 44:322-331.

Ramstein, G. and Raffy, M., 1989. Analysis of the structure of radiometric remotely-sensed images. *International Journal of Remote Sensing;* 10: 1049–1073.

Swift, M.J., Anderson, J.M., 1989. Decomposition. In: Lieth, H., Werger, M.J.A. (Eds.), Tropical Rain Forest Ecosystems. Biogeographical and Ecological Studies. Elsevier, Amsterdam, pp. 547–569.